PERGAMON

Chemical Engineering Science 55 (2000) 2379–2392

Chemical Engineering Science

Multiphase multicomponent equilibria for mixtures containing polymers by the perturbation theory

Federica Favari[a], Alberto Bertucco[a], Nicola Elvassore[a], Maurizio Fermeglia[b,*]

[a]*Istituto di Impianti Chimici, Università di Padova, via Marzolo 9, I-35131 Padova, Italy*
[b]*Dipartimento di Ingegneria Chimica, Ambiente e Materie Prime, Università di Trieste, Piazzale Europa 1, I-34127 Trieste, Italy*

Received 11 January 1999; accepted 23 September 1999

Abstract

The correlating and predictive capabilities of a thermodynamic model based on the perturbation theory are investigated, with reference to mixtures containing components of different size and molecular interactions. The simplified Perturbed-Hard-Sphere-Chain (PHSC) equation of state is applied to a series of pure polymers, a number of solvents and pure carbon dioxide, and both volumetric and equilibrium properties are considered. The ability of the proposed model to reproduce experimental phase equilibrium data is discussed and tested with reference to binary and multicomponent mixtures, in the presence of vapor–liquid, liquid–liquid and vapor–liquid–liquid equilibria. Attention is focused on the ternary system polystyrene–cyclohexane–carbon dioxide, to test the proposed thermodynamic model in view of simulating supercritical antisolvent-induced fractionation processes. It is shown that the PHSC equation of state can be reliably used for calculating the phase behavior of such a complex system in different conditions.

Keywords: Polymer systems; Vapor–liquid equilibria; Liquid–liquid equilibria; Vapor–liquid–liquid equilibria; PHSC EOS; Multi-component mixtures; Supercritical antisolvent separation

1. Introduction

As an answer to the cost reduction and the increasing efficiency of the polymer industry it is necessary to have a thermodynamic model able to describe the behavior of the mixtures in the widest range of operating conditions. This model, essentially used for describing phase equilibrium, is the most important tool of any process simulator, which in turn is a key tool in the modern chemical engineering profession. Examples of relevant industrial applications in this respect are the devolatilization of a solvent from a polymer solution, processes involving polymer blends and the new separation processes of a polymer–solvent mixture using supercritical solvents and antisolvents (SAS).

The SAS process is particularly interesting both from a practical and theoretical point of view (Bungert, Sadowski & Arlt, 1997). In practice, this separation technique may be successfully applied when thermal degradation of the polymer may occur if a traditional process is used. Basically, it uses the phase separation of a liquid polymer solution into a polymer-rich phase and a solvent-rich phase, which is almost polymer free. This phenomenon, which appears at elevated pressures by increasing temperature, according to the lower critical solution temperature behavior, can be obtained to lower temperatures by the addition of a compressed gas to a polymer–solvent system. This is so because the increased free volume of the solvent due to the supercritical additive is equivalent to the temperature effect in causing the high-temperature phase separation (Seckner, McClellan & McHugh, 1988). Solvent recovery processes from a polymer solution can then be carried out under less severe conditions, in terms of thermal stability of the polymer, and with less energetic demand.

To be useful for such complex industrial applications, the thermodynamic model that we need must be able to describe mixtures containing components with large differences in size and molecular interactions, in the simultaneous presence of two liquid and one vapor phases. It must be also able to reproduce all the different types of phase equilibria experimentally observed in these

* Corresponding author. Tel.: 0039-40-6763438; fax: 0039-40-569823.
E-mail address: mauf@dicamp.univ.trieste.it (M. Fermeglia)

0009-2509/00/$ - see front matter
PII: S0009-2509(99)00517-5

Nomenclature

a	equation of state parameter reflecting the attractive forces between two non-bonded segments, kPa cm^6/mol^2
a_p	equation of state attractive parameter for the polymer, kPa cm^6/mol^2
a_{ij}	equation of state parameter for the binary pair ij, kPa cm^6/mol^2
A^*	characteristic surface area, cm^2/mol
A_0^*	characteristic surface area of a polymer's molecule, cm^2/mol
b	Van der Waals covolume per segment, cm^3/mol
b_{ij}	equation of state parameter for the binary pair ij, cm^3/mol
d	hard-sphere diameter, Å
d_{ij}^+	ij-pair hard-sphere diameter, Å
E^*	characteristic cohesive energy, kJ/mol
E_0^*	characteristic cohesive energy of a polymer's molecule, kJ/mol
$f_i^{L_1}$	fugacity of component i in the polymer-rich liquid phase, kPa
$f_i^{L_2}$	fugacity of component i in the solvent-rich liquid phase, kPa
f_i^{V}	fugacity of component i in the vapor phase, kPa
F_a	universal function used to calculate $a(T)$
F_b	universal function used to calculate $b(T)$
$g(d^+)$	pair radial distribution function of hard spheres at contact
$g_{ij}(d_{ij}^+)$	ij-pair radial distribution function of hard spheres mixtures at contact
k	Boltzmann's constant, J/molcule K
k_{ij}	ij-pair interaction parameter
K_i	separation factors of components of the mixture
m	number of components of the mixture
M	molecular weight
M_0	molecular weight of the repeat unit of a polymer
M_i^{CALC}	calculated generic property for the ith datum
M_i^{EXP}	experimental generic property for the ith datum
n	number of experimental data used for the fitting procedure
N	number of molecules
N_A	Avogadro's constant, molecule/mol
N_i	number of the molecules of component i
NDAT	number of experimental data used for the fitting procedure
P	pressure, kPa
$P_i^{v,\mathrm{CALC}}$	pure component or mixture calculated vapor pressure for the ith datum, kPa
$P_i^{v,\mathrm{EXP}}$	pure component or mixture experimental vapor pressure for the ith datum, kPa
r	number of segments per molecule
r_i	number of segments for the ith component
r_p	number of segments for the polymer
r_p^*	corrected number of segments for the polymer
R_g	gas constant, J/mol K
RMSD	root mean square deviation
T	temperature, K
V	volume of the system, cm^3
V^*	characteristic volume, cm^3/mol
V_0^*	characteristic volume of a polymer's molecules, cm^3/mol
w_i	weights of the pure components properties used for data regression
x_i	number fraction of molecules
x_i	mole fractions of the components of the mixture in the polymer-rich phase
y_i	mole fractions of the components of the mixture in the solvent-rich phase
z_i	mole fractions of the components of the mixture in the feed

Greek characters

ε	depth of the minimum in the pair potential, J/mol
ΔM	percent mean relative deviation
ε_{ij}	ij-pair parameter ε, J/mol
η	packing fraction
v_B	corrective parameter for the polymer
$v_{\mathrm{Lsat},i}^{\mathrm{CALC}}$	pure component calculated saturated liquid volume for the ith datum, cm^3/mol
$v_{\mathrm{Lsat},i}^{\mathrm{EXP}}$	pure component experimental saturated liquid volume for the ith datum, cm^3/mol
ρ	Density,
ρ_r	segment-density of the polymer, cm^3/mol
ρ_i^{CALC}	pure component calculated single-phase density for the ith datum, mol/cm^3
ρ_i^{EXP}	pure component experimental single-phase density for the ith datum, mol/cm^3
σ	separation distance between segment centers at the minimum of the pair potential, Å
σ_{ij}	ij-pair parameter σ, Å
ϕ	ratio of the solvent-rich phase to the feed
φ_i	fugacity coefficient of component i in the mixture
φ_i^V	fugacity coefficient of component i in the vapor phase

systems, i.e. both the lower critical solution temperature (LCST) and the upper critical solution temperature (UCST) behavior.

Cubic equations of state are not useful to this aim, as was already shown by Fermeglia, Bertucco and Patrizio (1997). Also among the molecular-based thermodynamic models, the most commonly used Flory–Huggins theory (Flory, 1953) is not suitable to explain the complex liquid behavior displayed by polymer mixtures. One attempt of describing compressibility effects has been done by introducing the free volume concept in the Compressible-Lattice models (Sanchez & Lacombe, 1976,1978). Other variations of the Lattice-Fluid model have been developed (High & Danner, 1989,1990; Panayioutou & Vera, 1982) but all these theories ignore the continuos nature of the real polymer configurations. Recently, a number of statistical–mechanical equations of state, based on a more physically reasonable Continuous-Space theories of polymer mixtures have been developed (Chapman, Jackson & Gubbins, 1988; Chiew, 1990; Dickman & Hall, 1986; Honnel & Hall, 1989). In these relatively simple models, a molecule is represented by a series of freely jointed tangent hard spheres, the hard-sphere chain, which is able to take into account the complex phase behavior of real polymer systems including excluded volume effects and segment connectivity.

Among them is the perturbed hard-sphere chain (PHSC) equation of state, which is based on a modified Chiew equation of state for athermal hard-sphere chains. This model is applicable to fluids containing small or large molecules, because the effective hard-sphere diameter and attractive energy parameters are theoretically based functions of temperature (Song & Mason, 1991). Moreover, previous works (Song, Lambert & Prausnitz, 1994; Song, Hino, Lambert & Prausnitz, 1996) have demonstrated that the PHSC equation of state successfully reproduces all types of phase equilibria experimentally observed in binary mixtures containing polymers, including the lower critical solution temperature (LCST), the upper critical solution temperature (UCST), or both. Calculated liquid–liquid coexistence curves were found to be in good agreement with experiments for several binary mixtures containing polymers.

The primary purpose of this paper is to extend the use of the PHSC EOS to multicomponent mixtures containing molecules with large differences in size and interactions, and to describe with the same set of parameters a wide range of process conditions. In particular, this paper focuses on ternary systems containing polymer, solvent and antisolvent, because of the complexity of the phase behavior of these three-phase systems of recent industrial interest.

Although a systematic investigation of the influence of a supercritical fluid on the phase behavior of polymer systems has already been made (Irani & Cozewith, 1986; Seckner et al., 1988; Kennis, De Loos & De Swann Arons, 1990; Bungert et al., 1997) and the physical basis of observed experimental phenomena is well understood, experimental investigation in an extended range of temperature and composition have been carried out only recently. Furthermore, few systems have been experimentally considered and a complete characterization in terms of multicomponent systems is available only for the system polystyrene–cyclohexane–carbon dioxide system (Behme, Bungert, Sadowski & Arlt, 1998). As a consequence, we have considered this case as the reference system for showing how a new generation equation of state can help in solving the problem of phase equilibria calculations under wide process conditions in the presence of a complex phase behavior.

2. Theory

2.1. Pure components

The equation of state considered in this paper is the simplified PHSC EOS (Song et al., 1996). It takes the hard sphere chains as its reference system, in the form of the Chiew equation of state (Chiew, 1990), derived from the Percus–Yevick integral-theory coupled with chain connectivity (and modified by the introduction of the Carnahan–Starling radial distribution function of hard spheres at contact), and a van der Waals attractive term as the perturbation. The EOS in terms of pressure is the following:

$$\left(\frac{P}{\rho kT}\right) = 1 + r^2 b\rho g(d^+) - (r-1)[g(d+)-1] - \frac{r^2 a\rho}{kT}, \tag{1}$$

where P is the pressure, T the absolute temperature, $\rho = N/V$ the number density, N the number of molecules, V the volume of the system, k the Boltzmann's constant, d the hard-sphere diameter and $g(d+)$ the pair radial distribution function of hard spheres at contact. The three segment parameters r, a and b have all a direct physical meaning: r is the number of segments (hard spheres) per molecule, a reflects the attractive forces between two non-bonded segments and b is the Van der Waals covolume per segment. The effective hard sphere diameter b and the attractive-energy parameter a, according to the method of Song and Mason (1991), can be expressed in terms of constants associated with intermolecular forces, and be represented by two theoretically based functions of temperature:

$$a(T) = \frac{2\pi}{3}\sigma^3 \varepsilon F_a(kT/\varepsilon), \tag{2}$$

$$b(T) = \frac{2\pi}{3}\sigma^3 F_b(kT/\varepsilon), \tag{3}$$

where ε and σ are pair-potential parameters: ε is the depth of the minimum in the pair potential and σ is

the separation distance between segment centers at this minimum.

In Eqs. (2) and (3) F_a and F_b are expressed by empirical equations determined from thermodynamic properties of argon and methane over a large range of temperature and density:

$$F_a(kT/\varepsilon) = 1.8681 \exp\left[-0.0619\left(\frac{kT}{\varepsilon}\right)\right] + 0.6715 \exp\left[-1.7317\left(\frac{kT}{\varepsilon}\right)^{3/2}\right], \quad (4)$$

$$F_b(kT/\varepsilon) = 0.7303 \exp\left[-0.1649\left(\frac{kT}{\varepsilon}\right)\right] + 0.2697 \exp\left[-2.3973\left(\frac{kT}{\varepsilon}\right)^{2/3}\right]. \quad (5)$$

In summary, each pure component has three segment-based parameters: σ, ε and r, which can be combined to give a more useful set of parameters directly related to size, shape and energetic interactions of the molecules of the fluid considered. This may be done by defining a characteristic volume, V^*:

$$V^* = (\pi/6) r \sigma^3 N_A, \quad (6)$$

where N_A is Avogadro's constant; a characteristic surface area, A^*:

$$A^* = \pi r \sigma^2 N_A \quad (7)$$

and a characteristic "cohesive" energy, E^*:

$$E^* = r(\varepsilon/k) R_g, \quad (8)$$

where R_g is the gas constant.

The PHSC EOS for a pure polymer can be simplified further if the molecular weight is very high (as suggested by Song et al., 1996). If $\rho_r = r\rho$ is the segment-density of the polymer, Eq. (1) can be rewritten as

$$\left(\frac{P}{\rho_r kT}\right) = 1 + b\rho_r g(d^+) - \left(1 - \frac{1}{r}\right) g(d^+) - \frac{a\rho_r}{kT}. \quad (9)$$

For polymers, as long as r is large, one can neglect the $1/r$ term and use a simpler form of the equation:

$$\left(\frac{P}{\rho_r kT}\right) = 1 + b\rho_r g(d^+) - g(d^+) - \frac{a\rho_r}{kT}. \quad (10)$$

Moreover (Song et al., 1994), since both r and M (molecular weight) have high numerical values for polymers, the ratio r/M can be considered as a more representative parameter. Accordingly, the characteristic parameters of the pure fluid on a segment-basis become r/M, σ, ε; on a molecule basis we have

$$V_0^* = \pi/6 (r/M) M_0 \sigma^3 N_A, \quad (11)$$

$$A_0^* = \pi (r/M) M_0 \sigma^2 N_A, \quad (12)$$

$$E_0^* = (r/M)(\varepsilon/k) M_0 R_g. \quad (13)$$

where M_0 is the repeat unit's molecular weight.

2.2. Mixtures

Extension of Eq. (1) to mixtures is straightforward:

$$\frac{P}{\rho kT} = 1 + \rho \sum_{ij}^{m} x_i x_j r_i r_j b_{ij} g_{ij}(d_{ij}^+) - \sum_{i}^{m} x_i (r_i - 1)[g_{ii}(d_{ii}^+) - 1] - \frac{\rho}{kT} \sum_{ij}^{m} x_i x_j r_i r_j a_{ij}, \quad (14)$$

where $x_i = N_i/N$ is the number fraction of molecules, r_i the number of segments for the i-th component and $g_{ij}(d_{ij}^+)$ the ij-pair radial distribution function of hard sphere mixtures at contact. Because of the rigorously theoretical nature of the equation of state, no mixing rules are required for the reference term, and the attractive term only requires van der Waals one-fluid mixing rules. The mixture parameters a_{ij} and b_{ij} needed for each binary pair included in the mixture can be in fact obtained by extension of Eqs. (2) and (3):

$$a_{ij} = (2\pi/3)\sigma_{ij}^3 \varepsilon_{ij} F_a(kT/\varepsilon_{ij}), \quad (15)$$

$$b_{ij} = (2\pi/3)\sigma_{ij}^3 F_b(kT/\varepsilon_{ij}), \quad (16)$$

where F_a and F_b are defined by Eqs. (4) and (5). No combining rule is needed for σ as a consequence of the additivity of the hard-sphere diameters:

$$\sigma_{ij} = \frac{\sigma_{ii} + \sigma_{jj}}{2}. \quad (17)$$

For the energetic parameter ε we set

$$\varepsilon_{ij} = \sqrt{\varepsilon_i \varepsilon_j}(1 - k_{ij}), \quad (18)$$

where k_{ij} is one adjustable parameter introduced for each binary pair included in the mixture.

The required mathematical expression for $g_{ij}(d_{ij}^+)$ is given by the Boublik–Mansoori–Carnahan–Starling (BMCS) (Boublik, 1970; Mansoori, Carnahan, Starling & Leland, 1971) equation for hard-sphere mixtures:

$$g_{ij}(\eta, \xi_{ij}) = \frac{1}{1-\eta} + \frac{3}{2}\frac{\xi_{ij}}{(1-\eta)^2} + \frac{1}{2}\frac{\xi_{ij}^2}{(1-\eta)} \quad (19)$$

with

$$\eta = \frac{\rho}{4}\sum_{i}^{m} x_i r_i b_i, \tag{20}$$

$$\xi_{ij} = \left(\frac{b_i\, b_j}{b_{ij}}\right)^{1/3} \frac{\rho}{4}\sum_{k}^{m} x_k\, r_k\, b_k^{2/3}. \tag{21}$$

A summary of the development of the analytical expressions of all the properties of interest is reported by Fermeglia, Bertucco and Bruni (1998); here only the modifications to the model needed for describing liquid–liquid equilibria of polymer systems are described. Finally, one problem observed in applying the PHSC EOS to liquid–liquid equilibria of polymer solutions is that calculated LCST values are significantly lower than experimental. As suggested by Hino, Song and Prausnitz (1996), this is caused by the oversimplification of the perturbation term of the model, which neglects the radial distribution function and chain connectivity and is based on the mean field assumption, that fails for dilute polymer solutions such as those near the LCST. To take into account this observation, the empirical correction proposed by Hino et al. (1996) is introduced into the perturbation term of the PHSC EOS to reduce the polymer contribution $r_p^2 a_p$, representing the attractive interaction between two polymer molecules in a dilute solution. The correction is equivalent to the substitution of r_p with

$$r_p^* = r_p v_B \quad (v_b \leqslant 1), \tag{22}$$

i.e. to reduce the polymer's chain length, only in the perturbation term of the equation.

3. Calculation methods

3.1. Pure components

A set of three molecular parameters has been obtained by fitting experimental data for each pure component considered in this work. For pure volatile fluids the three molecular parameters V^*, A^* and E^* have been fitted to vapor pressure and saturated liquid density data as functions of temperature. For pure polymer liquids parameters V_0^*, A_0^* and E_0^* have been regressed from pressure–volume–temperature (PVT) data.

Details on the fitting procedure are given elsewhere (Fermeglia et al., 1998): the Levenberg–Marquardt algorithm, in the modification of the IMSL routine ZXSSQ, has been used to find a set of the three which minimizes the objective function OF defined as follows:

$$\mathrm{OF} = w_1\sum_i \frac{(P_i^{v,\mathrm{EXP}} - P_i^{v,\mathrm{CALC}})^2}{(P_i^{v,\mathrm{EXP}})^2} + w_2\sum_i \frac{(v_{\mathrm{Lsat},\,i}^{\mathrm{EXP}} - v_{\mathrm{Lsat},\,i}^{\mathrm{CALC}})^2}{(v_{\mathrm{Lsat},\,i}^{\mathrm{EXP}})^2} + w_3\sum_i \frac{(\rho_i^{\mathrm{EXP}} - \rho_i^{\mathrm{CALC}})^2}{(\rho_i^{\mathrm{EXP}})^2}. \tag{23}$$

Note that for pure polymers the properties considered are only single phase PVT data, while for pure volatile fluids they include also the vapor pressure and the saturated liquid volume, weighted according to w_i. The best parameters were determined by fitting Eq. (1) or Eq. (10) for pure volatile fluids and for polymers, respectively, to the pure component properties.

The algorithms used for calculating the density and the pure component equilibrium from Eqs. (1) and (10) can be found in Patrizio (1995).

3.2. Mixtures

Mixture calculation algorithms are described according to the particular phase behavior.

3.2.1. Vapor–liquid equilibrium

For each binary pair included in the multicomponent mixtures considered in this work, one binary interaction parameter (k_{ij}) was estimated by fitting binary vapor–liquid equilibrium (VLE) data. The fitting procedure used is described by Fermeglia et al. (1998), Bruni (1997) and by Favari (1998) and is based on the minimization of the following objective function:

$$\mathrm{OF} = \sum_{i=1}^{\mathrm{NP}} \left(\frac{P_i^{\mathrm{CALC}} - P_i^{\mathrm{EXP}}}{P_i^{\mathrm{EXP}}}\right)^2 \tag{24}$$

where NP is the number of equilibrium data for a given system. For each value of the binary parameter given by the external convergence algorithm, a bubble point calculation at constant temperature is performed to recalculate the objective function. Extension of the computer program to multicomponent mixtures has been developed to perform predictive bubble point calculations.

3.2.2. Liquid–liquid equilibrium

For binary mixtures of normal fluids no fitting procedure for determining the binary interaction parameter k_{ij} from liquid–liquid equilibrium (LLE) data was necessary since the binary interaction parameter obtained from VLE was directly used in flash calculations.

For binary mixtures containing polymers, parameters k_{ij} and v_B have been adjusted to match liquid–liquid equilibrium data, because extrapolation of their value from VLE data was not satisfactory.

A liquid–liquid isothermal flash calculation routine has been implemented for multicomponent mixtures of both normal fluids with polymers. In the first case, the Gibbs tangent plane stability test (Wasylkiewicz, Sridhar, Doherty & Malone, 1996) was used, following the Michelsen's approach (Michelsen, 1982a), to provide good initial estimates for the subsequent flash calculation. In the second case, good initial estimates of the LLE were generated starting far from the critical point,

where convergence is much faster and stable, and slowly approaching the critical zone.

The flash problem at constant temperature and pressure, if m is the number of components, requires the solution of a system of m equilibrium conditions, m material balances and a consistency constraint:

$$K_i(\mathbf{x}, \mathbf{y})x_i - y_i = 0, \tag{25}$$

$$(1 - \phi)x_i + \phi y_i - z_i = 0, \tag{26}$$

$$\sum_{i=1}^{m} x_i - \sum_{i=1}^{m} y_i = 0, \tag{27}$$

where ϕ is the ratio of the solvent-rich phase to the feed, x_i, y_i and z_i are the mole fractions of the components of the mixture, respectively, in the polymer-rich phase, in the solvent-rich phase and in the feed, K_i is the separation factor of the components of the mixture.

The system can also be rewritten as follows:

$$K_i = \varphi_i(\mathbf{x})/\varphi_i(\mathbf{y}), \tag{28}$$

$$x_i = z_i/\{1 + (K_i - 1)\phi\}, \tag{29}$$

$$y_i = K_i z_i/\{1 + (K_i - 1)\phi\}, \tag{30}$$

$$\sum_{i=1}^{m} z_i(K_i - 1)/\{1 + (K_i - 1)\phi\}, \tag{31}$$

where φ_i is the fugacity coefficient of component i in the mixture.

This system can be solved in a traditional fashion by direct substitution (Henley & Rosen, 1969; Michelsen, 1982b), but this procedure becomes unreliable for solutions with large-size differences between the solvent and the solute molecules since the K-factors are strongly composition dependent and gives rise to instability in the solution.

In this paper the flash equations were solved simultaneously by a Newton–Raphson iterative procedure with a decomposition algorithm (Chen, Duran & Radosz, 1993).

3.2.3. Vapor–liquid–liquid equilibria

The three-phase calculations performed in this work do not involve any parameter estimation procedure: only calculations at fixed parameters are presented.

For a ternary mixture, the specification of the temperature and the pressure of the system is sufficient to complete the definition of the problem. For a binary mixture, fixing the temperature saturates the degrees of freedom of the system, so the pressure must be considered a dependent variable such as the phase compositions. At a given temperature the numerical procedure implemented in this paper starts from the feed at the bubble point and performs a liquid–liquid flash calculation. The composition of the two liquid phases and a good initial estimate of the vapor phase composition (as shown below) is obtained. Subsequently, a bubble point calculation for the same initial feed providing the calculated vapor phase composition and the pressure of the system is carried out. If the resulting pressure does not agree, within the desired tolerance, with the previous assumption, the procedure is repeated, starting with the last value of the pressure. To generate a good initial estimate of the vapor-phase composition for the bubble point calculation, as suggested by Michelsen (1998), we consider that, at equilibrium, the following relationships between the fugacities in the three phases must be respected:

$$\ln f_i^V = \ln f_i^{L_1} = \ln f_i^{L_2}. \tag{32}$$

As a first approximation one can assume $\varphi_i^V = 1$ in evaluating Eq. (32). Defining the ratios W_i as

$$W_i = f_i^V/P = f_i^{L_1}/P = f_i^{L_2}/P \tag{33}$$

we obtain an estimate of the vapor phase composition as

$$y_i = W_i/\sum W_i \tag{34}$$

using the values of fugacities $f_i^{L_1}$ and $f_i^{L_2}$ previously determined by the liquid–liquid flash calculation.

4. Results

4.1. Pure components

Table 1 summarizes the 21 pure polymers investigated, along with the temperature and pressure range of the PVT data considered. The database used in this work is exactly the same as that of a previous paper (Song et al., 1994), where a previous version of the PHSC model was considered. Table 1 also reports the numerical values of parameters obtained by fitting the experimental data for pure polymers. The root-mean-square relative deviation (RMSD%) reported in Table 1 between calculated and experimental values is defined for a generic property M as

$$\mathrm{RMSD} = \frac{100}{n}\sum_i \sqrt{\frac{(M_i^{\mathrm{EXP}} - M_i^{\mathrm{CALC}})^2}{\mathrm{NDAT}(M_i^{\mathrm{EXP}})}}. \tag{35}$$

In Table 1, the RMSD% refers to density values calculated in the range of T and P reported in columns 2 and 3. Table 1 shows that the numerical values of RMSD is of the order of 0.04–0.5%, well within the experimental uncertainty.

Fig. 1 shows a comparison between the experimental data and the data calculated by means of the proposed method, by using the parameters reported in Table 1 for polystyrene.

Table 1
List of the pure polymers investigated along with the pressure and temperature range of the PVT data used. Columns 4–6 report the numerical values of the pure component parameters calculated in this work and the last column reports the RMSD % deviation in density relative to these parameters

Polymer	Pressure range (kPa)	Temperature range (K)	E^* (bar cm^3/mol)	A^* (10^9cm^2/mol)	V^* (cm^3/mol)	RMSD% (Eq. (35))
High-density poly ethylene (HDPE)	100. − 2.E + 5	415.25–472.85	37 383	3.8342	24.442	0.136
Low-density poly ethylene (LDPE)	0. − 1.E + 3	413.15–473.15	41 619	4.0272	24.242	0.143
Poly propylene (PP)	0. − 1.96E + 5	446.66–571.63	38 828	4.9885	39.117	0.228
Iso poly 1 butene (i-PB)	0. − 1.96E + 5	406.99–514.08	66 280	7.2485	49.770	0.273
Poly isobutene (PIB)	0. − 1.E + 5	325.95–383.15	76 826	7.3034	45.377	0.0828
Poly 4 methyl 1 pentane (PMP)	0. − 1.96E + 5	449.65–502.05	95 677	10.671	77.536	0.334
Poly styrene (PS)	1.E + 2 − 2.E + 5	388.55–468.75	128 880	110 529	74.483	0.133
Poly orto metylstirene (POMS)	1.E + 2 − 1.8E + 5	412.55–470.85	151 710	13.301	86.317	0.0904
Poly *cis* 1,4 butadiene (BR)	1.01E + 2 − 2.83E + 5	277.15–328.35	87 180	7.8358	43.303	0.0781
Poly vinyl chloride (PVC)	0. − 2.E + 5	373.35–423.15	71 398	5.658	33.372	0.174
Poly vinyl acetate (PVAC)	0. − 8.E + 4	308.15–373.15	108 240	3.4236	52.557	0.0409
Iso poly methyl metacrilate (i-PMMA)	1.E + 2 − 2.E + 5	290.35–432.15	130 390	10.357	63.23	0.144
Poly methyl metacrilate (PMMA)	1.E + 2 − 2.E + 5	386.65–432.15	134 480	10.581	62.519	0.0425
Poly butyl metacrilate (PBMA)	1.E + 2 − 2.E + 5	295.65–472.65	162 460	150 102	91.69	0.246
Poly cyclohexyl metacrilate (PHCMA)	1.E + 2 − 2.E + 5	382.75–472.05	188 690	160 709	105.65	0.127
Poly ethylene tereftalate (PETP)	0. − 1.96E + 5	551.45–615.45	276 240	19.099	106.65	0.383
Poly carbonate (PC)	0. − 1.77E + 5	429.88–610.01	301 810	24.048	148.74	0.195
Poly ether ether ketone (PEEK)	0. − 2.E + 5	619.35–670.95	367 250	27.584	165.94	0.456
Poly sulfone (PSF)	0. − 1.96E + 5	474.95–644.45	586 840	43.663	273.72	0.159
Poly tetrafluoro ethylene (PTFE)	0. − 3.92E + 4	603.55–645.55	48 573	5.3862	29.118	0.282
Poly tetra hydro furane (PT)	0. − 5.88E + 4	337.75–443.98	83 991	8.5731	54.77	0.126

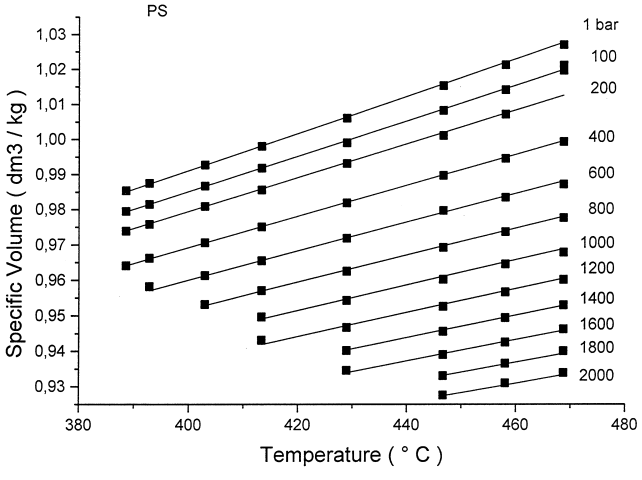

Fig. 1. PVT properties of polystyrene: comparison between experimental (symbols) and calculated (line) values by using the proposed method and the parameters reported in Table 1.

The pure component parameters for carbon dioxide are $V^* = 16.331$ cm^3/mol, $A^* = 4.1821{*}10^9$ cm^2/mol and $E^* = 42\,955$ bar cm^3/mol, in the validity range $P = 5.13$–7.36 kPa, $T = 216.6$–304.2 K. They have been determined by a multi-property regression method from subcritical vapor pressure data with a RMSD of 1.87%, and from supercritical density data, with a RMSD of 3.14%.

The physical meaning of the model parameters allows correlating them with the molecular structure. Expressions for the V_0^*, A_0^* and E_0^* parameters of the model have been developed as functions of the van der Waals area and volume, for V_0^* and A_0^*, and as a function of the cohesive energy, for E_0^* (Favari, 1998). As previously observed for the original model (Song et al., 1994), these correlations can provide estimates for EOS parameters of those polymers for which PVT data are unavailable. Since this paper focuses on multicomponent mixtures, the regressed pure component parameters reported in Table 1 will be used.

4.2. Binary mixtures

4.2.1. Vapor–liquid equilibrium

The systems investigated are summarized in Table 5 of the appendix, along with the literature references.

For components subcritical at the system temperature (except polymers) one vapor pressure datum at the same temperature has been used to recalculate the energetic parameter by constraining the calculated vapor pressure to be equal to the experimental one, thus avoiding any systematic shift in the pure component vapor pressure. In a previous paper it was shown that the performance of the model can be substantially improved by this procedure (Fermeglia et al., 1998).

In order to test the correlating capabilities of the model when applied to mixtures containing components

of different size, binary systems CO_2-solvent, polymer-solvent and CO_2-polymer have been considered. The solvent–solvent calculations presented here were performed to obtain the necessary interaction parameter for the multicomponent mixtures.

At a given temperature, for each binary pair, the k_{ij} parameter has been determined from the experimental VLE data referenced in Table 5. Table 2 reports the numerical value of the k_{ij} parameters obtained, along with the evaluation indexes RMSD (Eq. (35)) and % *m.r.d.* (*per cent mean relative deviation*), defined as follows:

$$\Delta M = \frac{100}{n}\left|\frac{M_i^{\mathrm{EXP}} - M_i^{\mathrm{CALC}}}{M_i^{\mathrm{EXP}}}\right|, \tag{36}$$

where M is a generic property and n is the number of experimental data considered.

In Table 2a, the marked systems (*) are those with only one subcritical component at the system temperature; in these cases the recalculation of the energetic parameter of the pure components has been performed only for the subcritical component. In Table 2b, we have indicated with (*) those systems on which the k_{ij} value has been fitted. In the case of the remaining systems a predictive calculation parameter has been performed, at the fixed value of k_{ij}.

Some correlation results are depicted in Fig. 2 for the CO_2–solvent systems.

The results reported in Table 2 allow to conclude that the binary interaction parameter increases with increasing molecular weight of the solvent, making it impossible to assume a single k_{ij} value for these systems, as can be made for binary mixtures of refrigerants and binary mixtures of hydrocarbons (Fermeglia et al., 1998). Furthermore, the binary interaction parameter shows an evident monotonically increasing k_{ij} dependence of temperature, that suggests the opportunity of a linearization of the parameter. A model correction to take into account for the quadrupole moment of the CO_2 is probably necessary.

Table 2
Binary interaction parameters, along with the corresponding evaluation indexes (Eqs. (35) and (36)); 2a: carbon dioxide–solvent systems; 2b: polymer–solvent systems; 2c: carbon dioxide$_2$ − polymer systems

System		T (K)	k_{ij}	% m.r.d p (Eq. (36))	RMSD y (Eq. (35))
2a:					
Carbon dioxide–methane	*	230	0.1215	3.81	0.03699
	*	270	0.1272	1.13	0.04309
Carbon dioxide–propane		244.26	0.1649	2.65	0.00894
		252.95	0.1610	2.06	0.02802
		266.48	0.1677	2.01	0.01095
		273.15	0.1888	3.44	0.01510
Carbon dioxide–*n.* pentane		277.65	0.1837	5.83	0.00496
	*	311.04	0.1852	3.49	0.00674
	*	344.15	0.1909	3.05	0.02260
	*	377.59	0.2021	3.28	0.03371
Carbon dioxide–*n.* hexane	*	313.15	0.1875	2.24	0.00358
	*	353.15	0.1957	3.22	0.08391
	*	393.15	0.2017	2.99	0.03113
Carbon dioxide–*n.* octane	*	313.15	0.1977	4.99	0.00245
	*	328.15	0.1969	3.17	0.00669
	*	348.15	0.1991	4.86	0.00828
Carbon dioxide–*n.* dodecane		298.15	0.1924	0.00418	0.00008
	*	308.15	0.1979	0.00406	0.00031
	*	318.15	0.2046	0.00396	0.00077
Carbon dioxide–*n.* eicosane	*	323.25	0.2003	2.13	0.00010
	*	373.45	0.2041	2.16	0.00009
	*	473.15	0.2219	1.76	0.00008
	*	573.15	0.2611	0.84	0.00248
Carbon dioxide–*n.* cyclohexane	*	344.3	0.2120	0.87694	0.04207

Table 2 (*continued*)

System		Molecular weight of polymer	T (K)	k_{ij}	% m.r.d.p (Eq. (36))
2b:					
PS–benzene		63 000 M_w	288.15	− 0.02569	7.28
		63 000 M_w	303.15	− 0.02569	3.92
		63 000 M_w	318.15	− 0.02569	4.43
	*	63 000 M_w	333.15	− 0.02569	3.84
PS–carbon tetrachloride	*	500 000 M_w	298.15	− 0.03532	4.41
PS–chloroform		1040 M_w	298.15	− 0.0242	7.67
	*	290 000 M_w	323.15	− 0.0242	1.59
PS–cyclohexane	*	150 000 M_n	297.85–329.45	− 0.03582	3.01
PIB–*n*. pentane		1350 M_w	298.15	− 0.05105	7.53
PVAC–chloroform	*	2700 M_w	298.15	− 0.05105	7.32
	*	194 000 M_w	333.15	− 0.02972	5.79
PMMA–chloroform	*	125 000 M_w	323.15	− 0.06097	3.59
BR-*n*. hexane	*	250 000 M_w	333.15	− 0.05219	0.832
BR–chloroform	*	250 000 M_w	333.15	− 0.02972	2.81
BR–cyclohexane	*	250 000 M_w	333.15	− 0.02035	3.59

System	Polymer molecular weight	T (K)	k_{ij}	% r.m.d. p (Eq. (36))	RMSD Y (Eq. (35))
2c:					
Carbondioxide–PS	187 000	373.2	0.1208	11.29	0.0
	187 000	413.2	0.1143	7.16	0.0
	187 000	453.2	0.1227	6.54	0.0

The results obtained for polymer–solvent systems confirm the good fitting capabilities of the PHSC EOS for this kind of systems, already shown elsewhere (Song et al., 1996; Hino et al., 1996), and the opportunity to assume for those mixtures a single value of k_{ij} with respect to temperature and to the polymer's molecular weight.

Finally, for the polystyrene–CO_2 system (Table 2c), the difficulty in the regression is evident and only a semi quantitative description of the system is possible.

4.2.2. Liquid–liquid equilibrium

Table 5 lists the binary LLE systems investigated, together with the corresponding literature references.

In order to test the capabilities of the model to reproduce the liquid–liquid equilibrium (LLE) of binary mixtures containing components with large differences in molecular size, CO_2–solvent and polymer–solvent systems have been considered.

For CO_2–solvent systems, calculations were performed using only one interaction parameter k_{ij}, determined from VLE data fitting. The binary interaction parameter of Table 2 has been linearized with respect to temperature in order to extrapolate its value to liquid–liquid equilibrium temperatures. Fig. 3 shows the acceptable agreement between calculated and experimental points for the system CO_2-dodecane.

Further calculations and sensitivity analysis with respect to the pressure and to the k_{ij} parameter are reported elsewhere (Favari, 1998).

For polymer–solvent systems calculations have been performed with reference to the polystyrene–cyclohexane system, already considered in literature (Hino et al., 1996). Using two adjustable parameters ($k_{ij} = 0.0179$ and $v_B = 0.739$), the theoretical coexistence curves agree fairly well with experimental data, also for systems which exhibit both an UCST and a LCST behavior (Favari, 1998).

4.2.3. Vapor–liquid–liquid equilibrium

The system CO_2–dodecane is considered as an example of binary vapor–liquid–liquid (VLLE) calculation. As for LLE, calculations have been performed using only one adjustable parameter k_{ij}, determined from VLE data fitting and extrapolated through the linearized function that relates k_{ij} to temperature. Fig. 4 presents three constant temperature VLE equilibrium curves, which exhibit, in a particular composition range, a liquid–liquid-phase separation. Increasing pressure, in such composition ranges, causes the vapor phase to disappear; decreasing temperature below the lowest value reported in Fig. 4 generates the separation of another solid phase, which cannot be represented by the model.

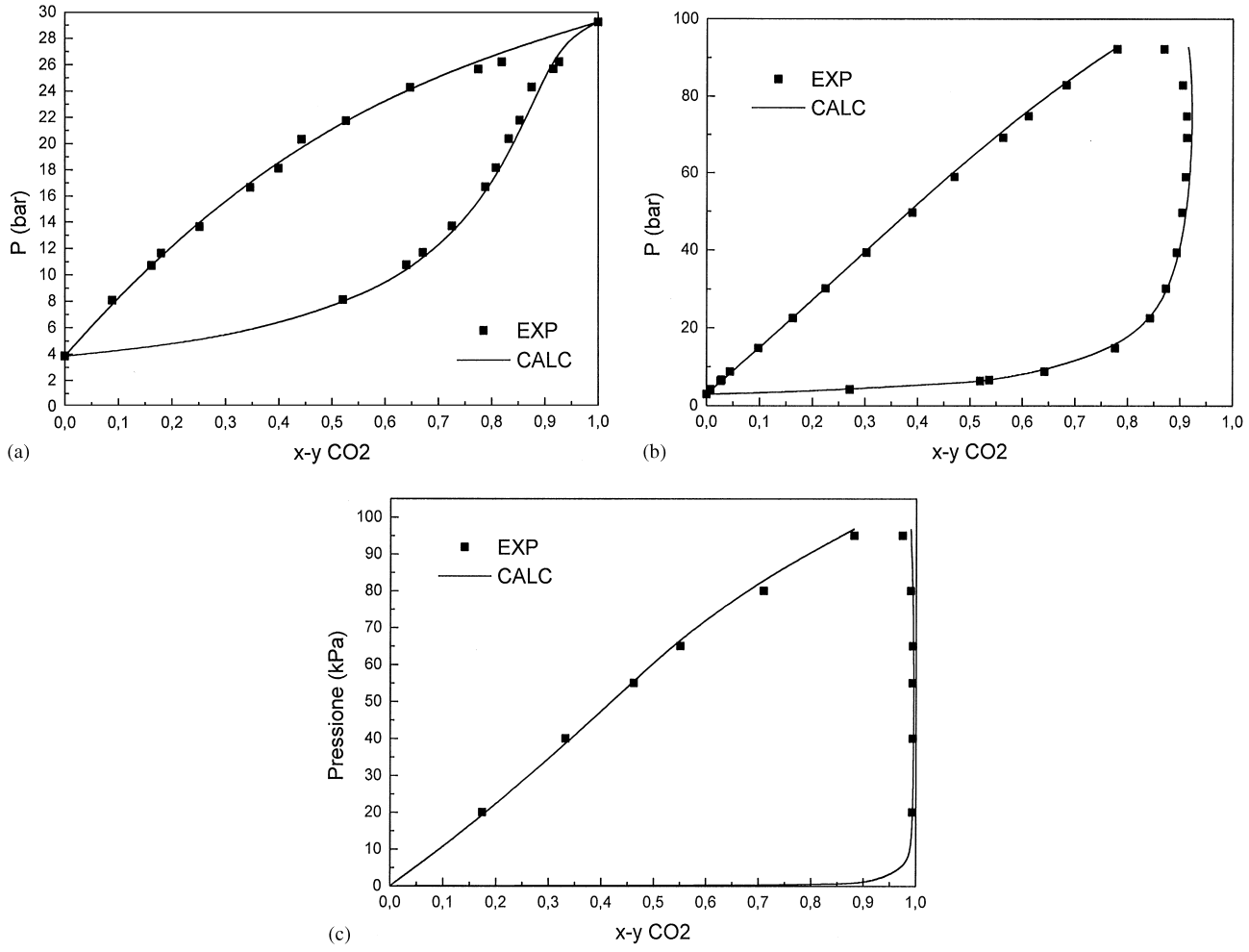

Fig. 2. VLE binary correlation results for systems carbon dioxide–solvent: a: carbon dioxide–propane system; $T = 266.48$ K; $k_{ij} = 0.1677$. b: carbon dioxide–*n*. pentane system; $T = 344.15$ K; k_{ij} 0.1909. c: carbon dioxide–*n*. octane system; $T = 328.15$ K; $k_{ij} = 0.1969$.

4.3. Multicomponent mixtures

4.3.1. Vapor–liquid equilibrium

Table 6 of the appendix lists the multicomponent systems investigated, along with the corresponding literature references. Calculations have been performed using only one adjustable parameter for each binary pair included in the mixture, determined from binary VLE data fitting. The multicomponent calculations can then be considered totally predictive. Tables 3 and 4 report the results obtained, respectively, for the systems C1–C3–C10 and CO_2–C3–C5–C8.

4.3.2. Liquid–liquid equilibrium

The ternary system polystyrene–cyclohexane–CO_2, for which experimental LLE and VLLE data are available (see Tables 5 and 6 for the reference), has been considered as a representative example of polymer–solvent-supercritical antisolvent system. As for all multicomponent calculations presented in this work, the binary interaction parameters have been determined by fitting binary data (LLE for the polystyrene–cyclohexane pair, VLE for the others). Therefore, the ternary

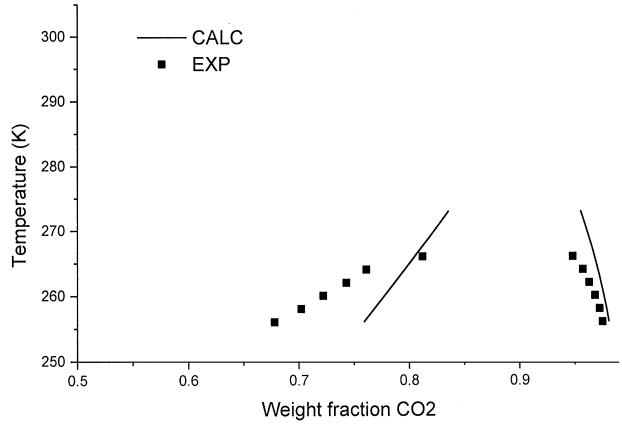

Fig. 3. LLE binary calculation results for system carbon dioxide–*n*. dodecane.

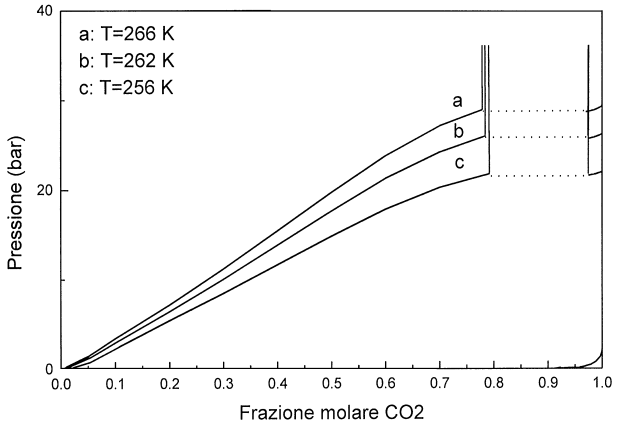

Fig. 4. VLLE binary calculation results for system carbon dioxide–*n*. dodecane.

Table 3
Multicomponent VLE calculation results for the methane–propane–*n*. decane system

T (K)	% m.r.d. p (Eq. (36))	RMSD y_1 (Eq. (35))	RMSD y_2 (Eq. (35))	RMSD y_3 (Eq. (35))
244.26	5.39	0.00543	0.00544	0.00001
255.37	5.07	0.00601	0.00602	0.00001
277.59	2.53	0.01058	0.01062	0.00006
294.26	2.03	0.00595	0.00607	0.00022

calculation can be considered fully predictive, and the corresponding results depend on the goodness of the binary data used.

The binary interaction parameters values have been determined as follows. For the polystyrene–cyclohexane pair, they were derived from LLE data and are those reported in the previous section of the paper. For the polystyrene–CO_2 system, the same value for the v_B parameter of the previous binary pair must be used to avoid discontinuity in the polystyrene behavior in the ternary mixture. The k_{ij} parameter has been readjusted by fitting it to the same VLE data presented in Table 5, at the fixed value of $v_B = 0.739$ (only the two temperatures $T = 413.2$ and 453.2 were considered for the fitting procedure, and the obtained k_{ij} value was linearized as a function of temperature, in order to extrapolate it to the LLE temperatures; the final value is 0.3786). For the CO_2–cyclohexane system, considering the increasing trend of k_{ij} with temperature for all the CO_2–solvent systems, a similar slope has been used for the extrapolation; the resulting value of k_{ij} for this binary pair is 0.24.

Fig. 5 compares theoretical equilibrium pressures, as a function of the two liquid-phase composition, with experimental data. We note that the PHSC EOS (as already demonstrated for the SAFT model, Behme et al., 1998) is able to represent at least qualitatively that a 2.6% rise in the total content of carbon-dioxide of the system has the same separation effect of an increase of 25°C in temperature; so, the same phase-separation process can be carried out under less severe conditions, in terms of polymer thermal degradation and of energetic expense.

4.3.3. *Vapor–liquid–liquid equilibrium*

Figs. 6 and 7 show the VLLE calculations performed for the same polymer–solvent-supercritical antisolvent system considered in the previous section, using the same model parameters. Fig. 6 compares the obtained theoretical phase diagram with experimental points. Using the same values of the pure component and of the binary parameters, the model is able to reproduce simultaneously four different regions of the phase-space of the

Table 4
Multicomponent VLE calculation results for the carbon dioxide$^{(1)}$–propane$^{(2)}$–*n*. pentane$^{(3)}$–*n*. octane$^{(4)}$ system

T (K)	p^{exp} (bar)	p^{calc} (bar)	y_1^{exp}	y_1^{cal}	y_2^{exp}	y_2^{calc}	y_3^{exp}	y_3^{calc}	y_4^{exp}	y_4^{calc}
310.93	30.8	31.44	0.6846	0.72949	0.2751	0.25307	0.0361	0.01709	0.00420	0.00035
310.93	32.5	32.79	0.6883	0.73855	0.2732	0.2732	0.0341	0.01653	0.00440	0.00035
310.93	34.2	34.34	0.7125	0.74771	0.2554	0.2554	0.0295	0.01594	0.00260	0.00035
324.82	35.8	36.37	0.6525	0.68590	0.2994	0.2994	0.0392	0.02480	0.00890	0.00074
324.82	37.8	38.83	0.6601	0.70036	0.2910	0.2910	0.0405	0.02359	0.00840	0.00074
324.82	40.0	41.03	0.6710	0.71240	0.2852	0.2852	0.0388	0.02268	0.00500	0.00074
338.71	41.6	41.38	0.6252	0.64154	0.3193	0.3193	0.0506	0.03431	0.00490	0.00148
338.71	44.4	43.91	0.6288	0.65498	0.3114	0.3114	0.0532	0.03298	0.00660	0.00147
338.71	47.3	47.40	0.6411	0.67227	0.3046	0.3046	0.0477	0.03160	0.00660	0.00148
352.59	47.8	49.08	0.5477	0.61537	0.3676	0.3676	0.0686	0.04509	0.01610	0.00278
352.59	50.6	51.95	0.5749	0.62407	0.3453	0.6453	0.0598	0.04371	0.02000	0.00276
352.59	54.5	49.87	0.5892	0.62500	0.3166	0.3166	0.0706	0.04080	0.02360	0.00313
366.48	53.1	53.27	0.5281	0.56752	0.3794	0.3794	0.0761	0.0553	0.01640	0.00491
380.7	58.2	59.67	0.4823	0.53399	0.4003	0.4003	0.0958	0.07430	0.02160	0.00843
349.26	63.7	64.76	0.4502	0.49327	0.4084	0.4084	0.1054	0.09172	0.02600	0.01367

Table 5
The system investigated are summarized along with the literature references

Solvent–solvent systems VLE	
Methane–Propane	Reamer, H. H., Sage B. H., & Lacey W. N. T. (1950). *Ind. Eng. Chem., 42*, 534
Methane–Hexane	Lin, Y., Chen, R. J. J., Chappelear, P. S., & Kobayashi, R. (1977). *J. Chem. Eng. Data, 22,* 402
Methane–Decane	Stalkup, F. I., & Kobayashi, R. (1963). *J. Chem. Eng. Data, 8,* 566
Propane–Pentane	Sage, B. H., & Lacey W. N. T. (1940). *Ind. Eng. Chem., 32,* 7
Propane–Octane	Ray, W. B., Genco, J., & Fichtner, D. A. (1974). *J. Chem. Eng. Data, 19,* 275
Propane–Decane	Reamer, H. H., & Sage, B. H. (1966). *J. Chem. Eng. Data, 11,* 18
Pentane–Octane	Chueh, P. L., & Prausnitz, J. M. (1967). *I & EC Fund., 6,* 492
Carbon tetrachloride–chloroform	Glashan, M. L., Prue, J. E., & Sainsbury, I. E. J. (1954). *Trans. Faraday Soc., 50,* 1284
Carbon dioxide–solvent VLE	
CO_2–Methane	Davalos, J., Anderson, W. R., Phelps R. E., & Kidnay, A. J. (1976). *J. Chem. Eng. Data, 21,* 81
CO_2–Propane	Nagahama, K., Konischi, H., Hoshino, D., & Hirata, M. (1974). *J. Chem. Eng. Jpn., 7,* 323
CO_2–Pentane	Besserer, G. J., & Robinson, D. B. (1973). *J. Chem. Eng. Data, 18,* 416
CO_2–Hexane	Li, Y., Dillard, K. H., & Robinson, R. L. Jr. (1981). *J. Chem. Eng. Data, 26,* 53
CO_2–Octane	Weng, N. L., & Lee, M. J. (1992). *J. Chem. Eng. Data, 37,* 213
CO_2–Dodecane	Hayduk, W., Walter, E. B., & Simpson, P. (1972). *J. Chem. Eng. Data, 17,* 59
CO_2–Eicosane	Huang, S. H., Lin, H., & Chao, K. (1988). *J. Chem. Eng. Data, 33,* 145
CO_2–Cyclohexane	Nagarajan, N., & Robinson, R. L. Jr. (1987). *J. Chem. Eng. Data, 32,* 36
Polymer–solvent systems VLE	
PS–Benzene	Noda, I., Higo, Y., Veno, N., & Fujimoto, T. (1984). *Macromolecules, 17,* 1055
PS–Carbon tetrachloride	Baughan, E. C. (1948). *Trans. Faraday Soc., 44,* 495
PS–Chloroform	Bawn, C. E. H., & Wajid, A. A. (1956). *Trans. Faraday Soc., 52,* 1658 + Panayiotou, C., & Vera, J. H. (1984). *Polym. J., 16,* 89
PS–Cyclohexane	Schmoll, K., & Jenckel, E. (1956). *Z. Elektrochem., 60,* 756
PVAC–Chloroform	Gupta, R. B., & Prausnitz, J. M. (1995). *J. Chem. Eng. Data, 40,* 78
PMMA–Chloroform	Tanbonliong, J. O., & Prausnitz, J. M. (1997). *Polymer, 38,* 5775
BR–Hexane	Gupta, R. B., & Prausnitz, J. M. (1995). *J. Chem. Eng. Data, 40,* 78
BR–Cyclohexane	Gupta, R. B., & Prausnitz, J. M. (1995). *J. Chem. Eng. Data, 40,* 78
PIB–Pentane	Panayiotou, C. G., & Vera, J. H. (1984). *Polym. J., 16,* 89
BR–Chloroform	Gupta, R. B., & Prausnitz, J. M. (1995). *J. Chem. Eng. Data, 40,* 78
Carbon dioxide–polymer systems VLE	
CO_2–PS	Sato, Y., Yurugi, M., Fujiwara, K., Takishima, S., & Masuoka, H. (1996). *Fluid Phase Equilibria, 125,* 129
Carbon dioxide–solvent systems LLE and VLLE	
CO_2–Dodecane	Hottovy, J. D., Luks, K. D., & Kohn, J. P. (1981). *J. Chem. Eng. Data, 26,* 256
CO_2–Eicosane	Huie, N. C., Luks, K. D., & Kohn, J. P. (1973). *J. Chem. Eng. Data, 18,* 311
Polymer–solvent systems LLE	
PS–Benzene	Saeki, S., Kuwahara, N., Konno, S., & Kaneko, M. (1973). *Macromolecules, 6,* 589
PS–Cyclohexane	Saeki, S., Kuwahara, N., Konno, S., & Kaneko, M. (1973). *Macromolecules, 6,* 246

Table 6
Multicomponent systems investigated

Solvent–solvent–solvent systems VLE	
Methane–Propane–Decane	Koonce, K. T., & Kobayashi, R. (1964). *J. Chem. Eng. Data, 11,* 18
Carbon dioxide–solvent–solvent systems VLE	
CO_2–Propane–Pentane–Octane	Barrufet, M. A., & Rahman, S. (1977). *J. Chem. Eng. Data, 42,* 120
Polymer–solvent–solvent systems VLE	
Polystyrene–Carbon Tetrachloride–Chloroform	Tanbonliong, J., & Prausnitz, J. M. (1997). *Polymer, 38,* 5775
Carbon dioxide–solvent–polymer systems LLE and VLLE	
CO_2–Cyclohexane–polystyrene	Bungert, B., Sadowski, G., & Arlt, W. (1997). *Fluid Phase Equilibria, 139,* 349

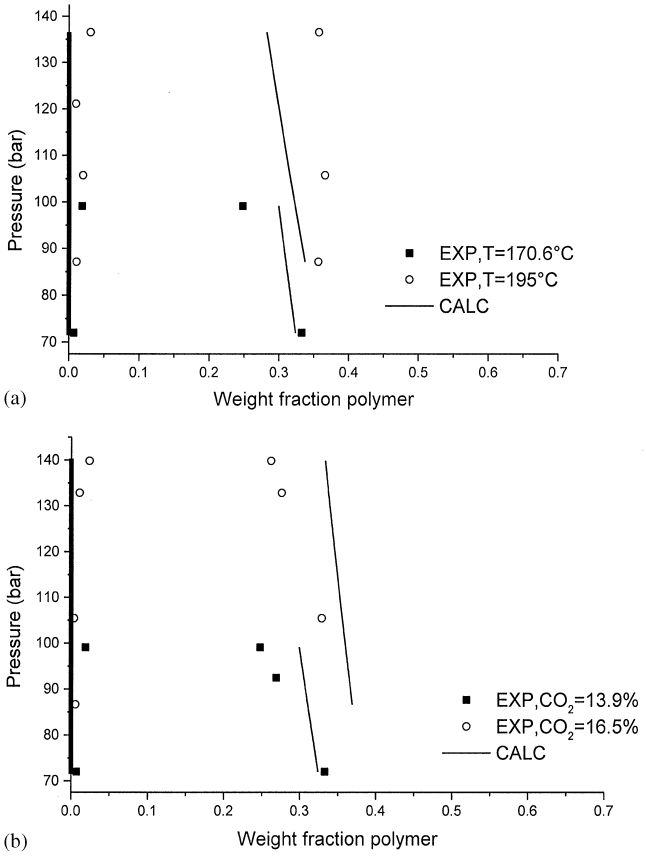

Fig. 5. LLE ternary calculation results for system polystyrene–cyclohexane–carbon dioxide: a: fixed CO_2 percentage = 13.9%. b: fixed temperature = 170.6°C.

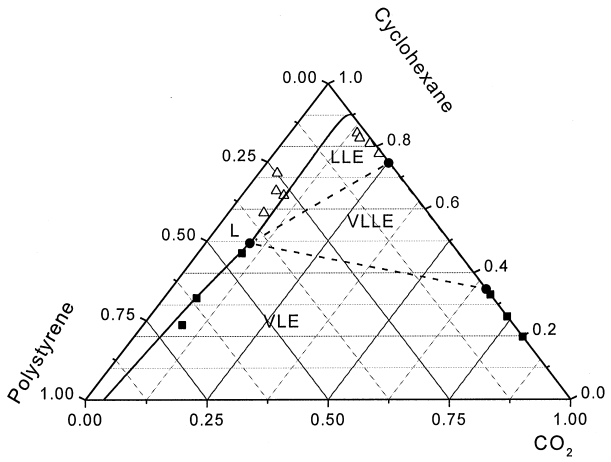

Fig. 6. VLLE ternary calculation results for system polystyrene–cyclohexane–carbon dioxide: $T = 170°C$; $P = 101$ bar.

mixture: the VLE zone, in the lower part of the diagram, the liquid zone, which includes the polystyrene–cyclohexane binary pair, the LLE zone, in the upper part of the diagram, and the VLLE zone, in the centre of the

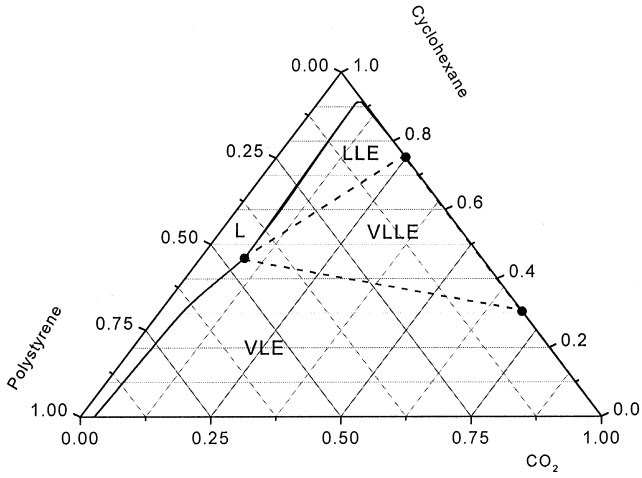

Fig. 7. VLLE ternary calculation results for system polystyrene–cyclohexane–carbon dioxide: $T = 170°C$; $P = 70$ bar.

triangle. A mixture of composition **z** included in this zone, splits into one vapor phase, practically solvent free, and two liquid phases, one solvent-rich and a second one, which contains more than 40% by weight of polymer. This phase separation appears under temperature and pressure conditions at which the polystyrene–cyclohexane system forms only one stable liquid phase and is allowed by the introduction of less then 25% weight of CO_2 in the mixture.

Finally, Fig. 7 investigates, in a predictive framework, the effect of pressure on this phase separation. These results cannot be compared to experimental data, that are unavailable for the considered conditions. Decreasing pressure facilitates the phase separation, because the differences in the free volume of the mixture's components, that are responsible for the high-temperature phase separation, are enhanced. Therefore, following the model prediction, the process could be carried out under milder conditions.

5. Conclusions

The simplified PHSCT model has been applied to pure polymers and to mixtures of polymers, solvents and supercritical fluids with the aim of investigating its correlating and predictive capabilities in the description of the complex phase behavior of such systems.

The results obtained show clearly that the model is able to describe such systems in a qualitative and semi-quantitative way.

Specifically, for pure polymers good calculations can be made, which lie within the experimental uncertainty of the data.

For binary systems vapor–liquid equilibrium calculations results are also good as far as the correlation of

experimental data is concerned. For polymer–solvent systems also the value of the binary interaction parameter is quite stable and not depending on temperature. This is not the case for CO_2–solvent systems, where a correction to the model is necessary. As far as the liquid–liquid and the vapor–liquid–liquid calculations are concerned, good predictive capabilities of the model can be found for CO_2–solvent systems. The model can also reproduce both the upper critical solution temperature and the lower critical solution temperature behavior of the polymer–solvent systems.

For ternary and multicomponent systems vapor–liquid and liquid–liquid predictive calculations agree fairly well with experiment.

Multiphase multicomponent system behavior for the only system available for investigation gave excellent results and the model proved to be an interesting tool for the prediction of phase behavior in different conditions.

Acknowledgements

The authors wish to thank J.M. Prausnitz for his helpful suggestions and the Ministero dell'Università e della Ricerca Scientifica (MURST — Roma) for the financial support.

References

Behme, S., Bungert, B., Sadowski, G., & Arlt, W. (1998). Separation of polymer systems by compressed gases: Experimental results and correlation. *Eighth international conference on properties, phase equilibria for product and process design*, Noordwijkerhout, The Netherlands, April 26th–May 1st.

Boublik, T. J. (1970). Hard-sphere equation of state. *Chemical Physics*, *53*, 471.

Bruni, S. (1997). *Tesi di Laurea*, University of Padova.

Bungert, B., Sadowski, G., & Arlt, W. (1997). Supercritical antisolvent fractionation: Measurements in the systems monodisperse and bidisperse polystyrene–cyclohexane–carbon dioxide. *Fluid Phase Equilibria*, *139*, 349.

Chapman, W. G., Jackson, G., & Gubbins, K. E. (1988). Statistical thermodynamics of *r*-mer fluid and their mixtures. *Polymer Journal*, *14*, 681.

Chen, C. K., Duran, M. A., & Radosz, M. (1993). Phase equilibria in polymer solutions. Block-algebra, simultaneous flash algorithm coupled with SAFT equation of state, applied to single-stage supercritical antisolvent fractionation of polyethylene. *Industrial and Engineering Chemistry Research*, *32*, 3123.

Chiew, Y. C. (1990). Percus–Yevick Integral equation theory for athermal hard-sphere chains. *Molecular Physics*, *70*, 129.

Dickman, R., & Hall, C. K. (1986). Equation of State for Athermal Chains. *Journal of Chemical Physics*, *90*, 1841.

Favari, F. (1998). *Tesi di Laurea*. University of Padova.

Fermeglia, M., Bertucco, A., & Bruni, S. (1998). A perturbed hard sphere chain equation of state for applications to hydrofluorocarbons, hydrocarbons and their mixtures. *Chemical Engineering Science*, *53*, 1.

Fermeglia, M., Bertucco, A., & Patrizio, D. (1997). Thermodynamic properties of pure hydrofluorocarbons by a perturbed hard-sphere-chain equation of state. *Chemical Engineering Science*, *52*, 1517.

Flory, P. J. (1953). *Principles of polymer chemistry*. Ithaca: Cornell University Press.

Henley, E. F., & Rosen, E. M. (1969). *Material and energy balance computations*. New York: Wiley.

High, M. S., & Danner, R. P. (1989). A group contribution equation of state for polymer solutions. *Fluid Phase Equilibria*, *53*, 323.

High, M. S., & Danner, R. P. (1990). Application of the group contribution lattice-fluid EOS to polymer solutions. *AIChE Journal*, *36*, 1625.

Hino, T., Song, Y., & Prausnitz, J. M. (1996). Liquid–liquid equilibria and theta temperatures in homopolymer-solvent solutions from a perturbed hard-sphere-chain equation of state. *Journal of Polymer Science*, *34*, 1961.

Honnel, K. G., & Hall, C. K. (1989). A new equation of state for chain molecules: Continuos-space analog of flory theory. *Journal of Chemical Physics*, *85*, 4108.

Irani, C. A., & Cozewith, C. (1986). Lower critical solution temperature behaviour of ethylene propylene copolymers in multicomponent solvents. *Journal of Applied Polymer Science*, *31*, 1879.

Kennis, H. A. J., De Loos, T. H. W., & De Swann Arons, J. (1990). The influence of nitrogen on the liquid–liquid phase behaviour of the system *n*-hexane-polyethylene: Experimental results and predictions with the mean-field lattice-gas model. *Chemical Engineering Science*, *45*, 1875.

Mansoori, G. A., Carnahan, N. F., Starling, K. E., & Leland, T. W. (1971). Equilibrium thermodynamic properties of the mixture of hard sphere. *Journal of Chemical Physics*, *54*, 1523.

Michelsen, M. K. (1982a). The isothermal flash problem. Part 1. Stability. *Fluid Phase Equilibria*, *9*, 1.

Michelsen, M. L. (1982b). The isothermal flash problem. Part 2. Phase-split calculation. *Fluid Phase Equilibria*, *9*, 21.

Michelsen, M. L. (1998). personal communication.

Panayioutou, C., & Vera, J. H. (1982). Statistical thermodynamics of *r*-mer fluid and their mixtures. *Polymer Journal*, *14*, 681.

Patrizio, D. (1995). *Tesi di Laurea*. University of Padova.

Sanchez, I. C., & Lacombe, R. H. (1976). Statistical thermodynamics of fluid mixtures. *Journal Physical Chemistry*, *80*, 2568.

Sanchez, I. C., & Lacombe, R. H. (1978). Statistical thermodynamics of polymer mixtures. *Macromolecules*, *11*, 1145.

Seckner, A. J., McClellan, A. K., & McHugh, M. A. (1988). High-pressure solution behavior of the polystyrene–toluene–ethane system. *AIChE Journal*, *34*, 9.

Song, Y., & Mason, E. A. (1991). Statistical–mechanical theory of a new analytical equation of state. *Journal of Chemical Physics*, *12*, 7840.

Song, Y., Hino, T., Lambert, S. M., & Prausnitz, J. M. (1996). Liquid–liquid equilibria for polymer solutions and blends, including copolymers. *Fluid Phase Equilibria*, *117*, 69.

Song, Y., Lambert, S. M., & Prausnitz, J. M. (1994). Liquid–liquid phase diagrams for binary polymer solutions from a perturbed-hard-sphere-chain equation of state. *Chemical Engineering Science*, *49*, 2765.

Wasylkiewicz, S. K., Sridhar, L. N., Doherty, M. F., & Malone, M. F. (1996). Global stability analysis and calculation of liquid–liquid equilibrium in multicomponent mixtures. *Industial and Engineering Chemistry Research*, *35*, 1395.